

# Experimental evaluation of energy dissipation and viscous damping of repaired and strengthened RC columns with CFRP jacketing under biaxial load



Hugo Rodrigues<sup>a,\*</sup>, André Furtado<sup>b</sup>, António Arêde<sup>b</sup>

<sup>a</sup>RISCO, School of Technology and Management, Polytechnic Institute of Leiria

<sup>b</sup>CONSTRUCT-LESE, Faculty of Engineering (FEUP), University of Porto, Portugal

## ARTICLE INFO

### Article history:

Received 8 July 2016

Revised 27 April 2017

Accepted 10 May 2017

Available online 18 May 2017

### Keywords:

RC strengthened columns

RC repaired columns

CFRP jacketing

Energy dissipation

Damping

## ABSTRACT

The seismic repair and retrofitting of reinforced concrete (RC) columns have been the focus of innumerable studies and from the literature it can be concluded that the biaxial horizontal loading can reduce considerably the strength capacity, ductility and energy dissipation of the columns when compared with the corresponding response to uniaxial loading tests. However, reduced information regarding the influence of the retrofit strategies in the energy dissipation capacity and the viscous damping of the columns were obtained. Thus the main goal of the present work is to evaluate the efficiency of the Carbon Fiber Reinforced Polymer (CFRP) jacketing technique to improve the behaviour of three damaged columns subjected to repair procedures and four “as built” columns behaviour and evaluate their influence in the energy dissipation capacity and viscous damping of the columns when compared with the original response. From the test results a good efficiency of the CFRP jacketing improved about 20% the original energy dissipation capacity. Regarding the viscous damping it was obtained about 10% lower values for the repaired columns and to 20% higher values for the strengthened ones.

© 2017 Elsevier Ltd. All rights reserved.

## 1. Introduction

The structural behaviour of reinforced concrete (RC) columns subjected to biaxial cyclic loading combined with constant or variable axial load is very important to characterize the response of the existing and new buildings located in earthquake prone regions. From the experimental tests available in the literature, it was observed that the maximum strength in one specific direction of the columns, for each biaxial test against the corresponding uniaxial test, lower values were obtained for all biaxial tests than uniaxial ones, namely in terms of maximum strength in their weak direction, while smaller reductions for the stronger direction. It was also observed that the biaxial tests dissipated more energy than the uniaxial tests, however the viscous damping depends of the load path [1–4].

The fundamental parameters governing the structural response of the structural elements when subjected to seismic actions are: strength, stiffness, energy dissipation, damping and ductility. The study of different retrofit strategies has been performed during the last years. The most common retrofit techniques are [5–10]:

RC columns jacketing [11–14], steel jacketing [15,16], injection of epoxy resin [17], shotcrete and the Carbon Fiber Reinforced Polymer (CFRP) plates jacketing [18–23].

The RC columns energy dissipation capacity is of full importance for a satisfactory seismic response of the structures. For structures designed to accommodate levels of damage without collapse due to an earthquake, the input energy can be dissipated through their RC elements. Non-linear static methods are used on the assessment and design based on the energy dissipation capacity of the elements, that evaluate their seismic response, or particular parameters such as stiffness and/or strength degradation. For this, the viscous damping is used to characterise the energy dissipation capacity of the RC columns. The displacement based design (DBD) method [24] use the concept of the substitute-structure, which represents the structure intended for design or assessment purposes by the secant stiffness to maximum displacement response and equivalent viscous damping representing the combined effects of elastic and hysteretic damping [25]. Energy dissipation and the equivalent viscous damping are correlated with displacement ductility for uniaxial stress.

The main objective of the present work is to compare the energy dissipation and equivalent viscous damping between two groups of RC columns repaired and strengthened with CFRP jacket-

\* Corresponding author.

E-mail address: [hugo.f.rodrigues@ipleiria.pt](mailto:hugo.f.rodrigues@ipleiria.pt) (H. Rodrigues).

ing: i) three repaired RC columns with CFRP jacketing and ii) four strengthened “as built” columns with CFRP plates subjected to biaxial cyclic bending and constant axial load. Along the manuscript the experimental results will be focused in the energy dissipation and damping capacity of the columns under study. In particular, the energy dissipation of all the specimens was evaluated in terms of individual cycle dissipated energy, cumulative energy dissipation and equations regarding the normalized energy dissipation relating with the displacement ductility are proposed for each group of columns studied. Finally, the equivalent viscous damping was determined for each specimen comparing the influence of the CFRP jacketing in the RC columns response under biaxial loadings. It will be evaluated and discussed equations proposals for estimate the equivalent viscous damping proposed by different authors and simplified expressions will be proposed for repaired and strengthened RC columns with CFRP jacketing technique.

## 2. Experimental investigation

### 2.1. Specimen description and loading condition

The experimental campaign carried out for the present study was performed at the Laboratory of Earthquake and Structural Engineering (LESE). Ten rectangular RC columns were subjected to cyclic biaxial flexure (under two different horizontal displacement pattern) combined with constant axial load. The specimens have the same cross-section  $0.30 \times 0.50 \text{ m}^2$  and 1.70 m height, with longitudinal and transversal reinforcement detailing composed by  $14\phi 12$  mm and  $\phi 6//0.15$  m (illustrated in Fig. 1). The specimens under studied were selected from two different experimental campaigns, namely from the studies [5,6]. The studies carried out with the goal of evaluate the efficiency of different retrofit techniques to restore and/or improve the columns strength, initial stiffness and ductility capacity of columns repaired and strengthened. From the Ref. [6] it was selected the specimens that compose Group R, and from the Ref. [5] was selected the specimens that compose group S. The main considerations of each specimens group are described below:

- Group R: 4 RC columns with the same geometric dimensions, reinforcement detailing and material characteristics were tested for the same loading history (biaxial flexure with the horizontal displacement path diagonal  $45^\circ$  and axial load of 300kN). The group is composed by one as built column and three columns previously damaged and repaired retrofitted with CFRP jacketing technique;
- Group S1 and S2: 6 RC columns with the same geometric dimensions, reinforcement detailing, were tested for two different loading histories: biaxial flexure with the horizontal displacement path diagonal  $45^\circ$  and diamond combined with 300kN axial load. The group is composed by two original specimens and four strengthened columns with CFRP jacketing technique. The specimens subjected to the diagonal  $45^\circ$  horizontal displacement path (PC12-N13 and PC12-N17S) compose the group S1 and the remaining ones compose the Group S2 (PC12-N14, PC12-N10S, PC12-N12S and PC12-N18S).

Details of the reinforcement and material properties, horizontal displacement path, axial load and repair/strengthening technique are summarized in Table 1. The horizontal displacement paths are illustrated in Fig. 2.

For each lateral displacement demand level, three cycles were repeated. The following nominal peak displacement levels (in mm) were considered: 3, 5, 10, 4, 12, 15, 7, 20, 25, 30, 35, 40, 45, 50, 55, 60, 65, 70, 75, 80.

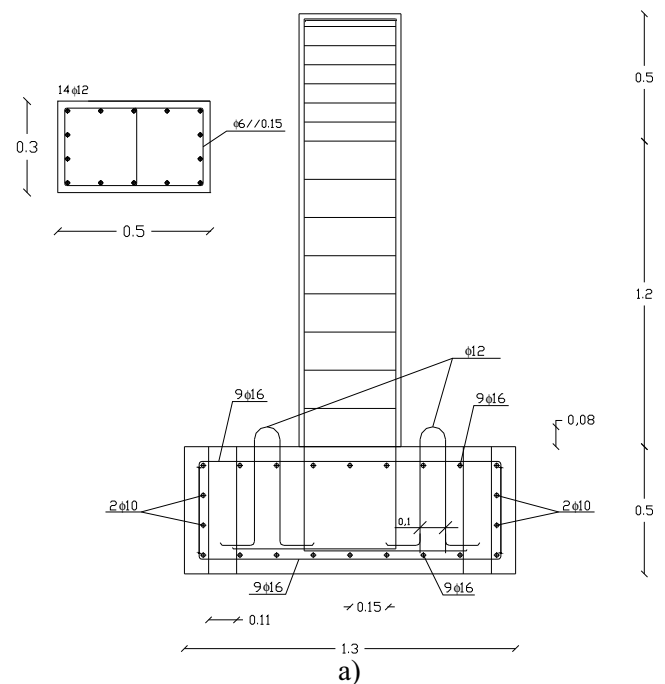


Fig. 1. a) RC column specimen dimensions and reinforcement detailing; b) General view of the test specimen at LESE laboratory.

### 2.2. Repair and retrofit process

#### 2.2.1. Group R

The previously damaged RC columns were subjected to repair procedures that can be resumed in five stages:

- Definition of the area that will be repaired (in the present work the repair area was defined as the critical section at the plastic hinge region), typically from the footing up to 50 cm along the column height) – Stage 1;
- Removal and cleaning of the damaged concrete;
- The repair procedure of the longitudinal reinforcement rebars (Stage 2) was performed by welding process and started by use discontinuous welding of the two sides, being the splicing of the interior steel rebars in a perpendicular plane to the faces of the column (Fig. 3c). This splicing position is the most suitable for the solution composed by the welding of two sides.

**Table 1**  
Specimen specifications and loading characteristics.

Group	Specimen	Geometry [cm × cm]	$f_{cm}$ [MPa]	$f_{yk}$ [MPa]	Axial Load [kN]	Horizontal displacement path type	Strengthening technique
R	PC12-N05 PC12-N04R PC12-N05R PC12-N07R	30 × 50	23.3	478	300	Diagonal – 45°	As built CFRP sheet jacketing CFRP plates jacketing
S1	PC12-N13		14.8	575.6		Diagonal – 45°	As built
S2	PC12-N14 PC12-N10S PC12-N12S		8.4	573.7		Diamond	As built CFRP plates jacketing
S1	PC12-N17S		14.8	575.6		Diagonal – 45°	
S2	PC12-N18S					Diamond	

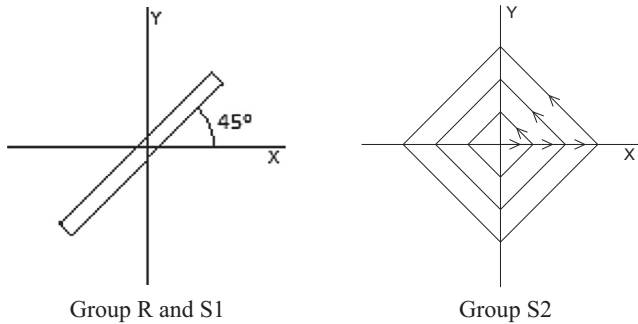


Fig. 2. Horizontal displacement paths types.

The 14 pieces required for the fourteen longitudinal steel rebars were prepared and were welded to the longitudinal rebars of the foundation, as can be observed in Fig. 3d.

- Finished this stage, the column was lined up according to the welded steel rebars, followed by the final welding process between them and the columns steel rebars: starting from the lateral weld splicing followed by the opening of the chamfer for posterior realization of the butt welding;
- Replacement of the transversal reinforcement with the half of the initial space of 0.15 m – Stage 3 (Fig. 4a);
- Application of a wood formwork and concreting with new micro-concrete to restore the previously sanitized area of the column – Stage 4 (Fig. 4b);

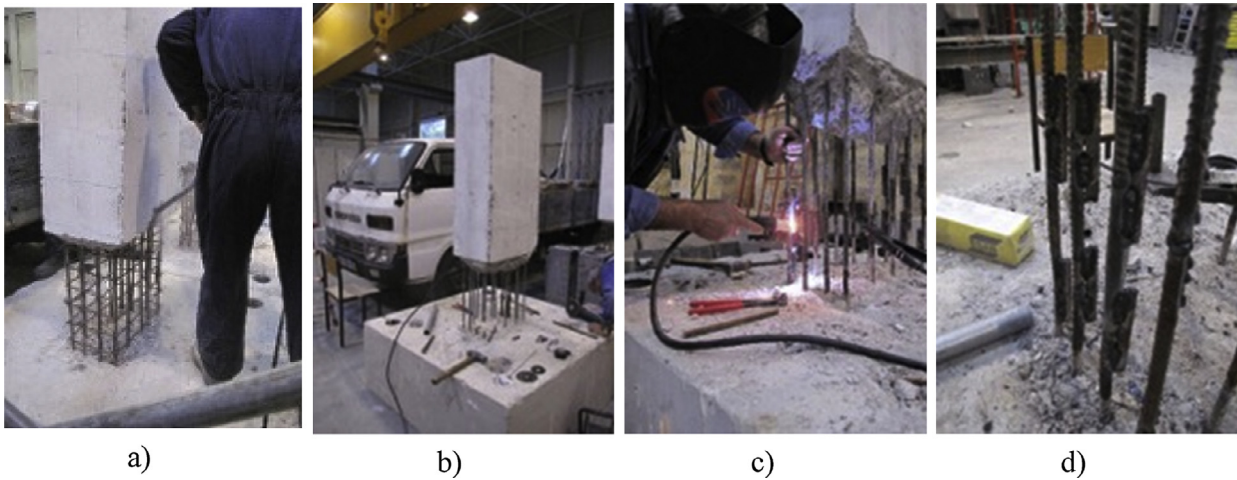


Fig. 3. Repair and retrofit strategies of RC columns a) and b) Stage 1; c) and d) Stage 2.

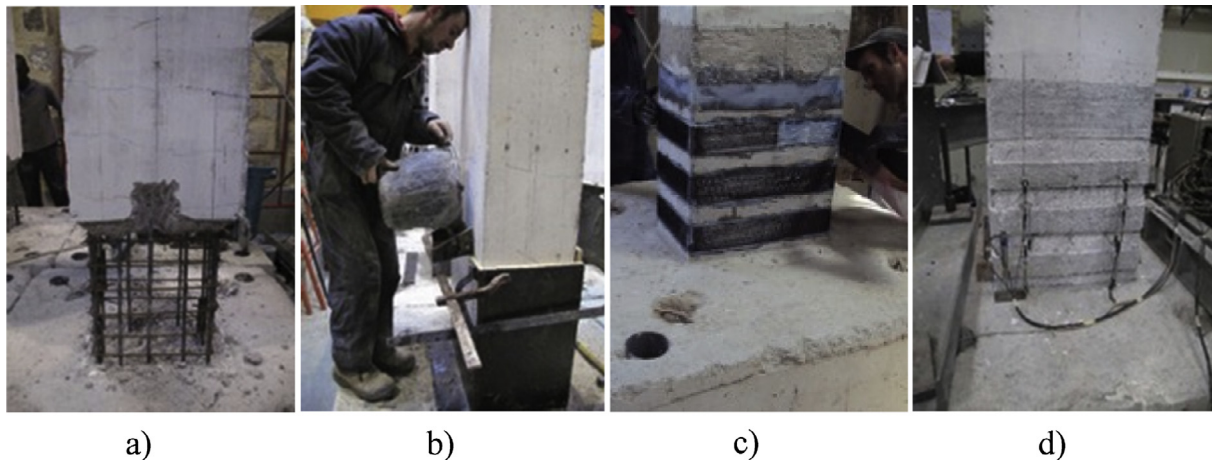
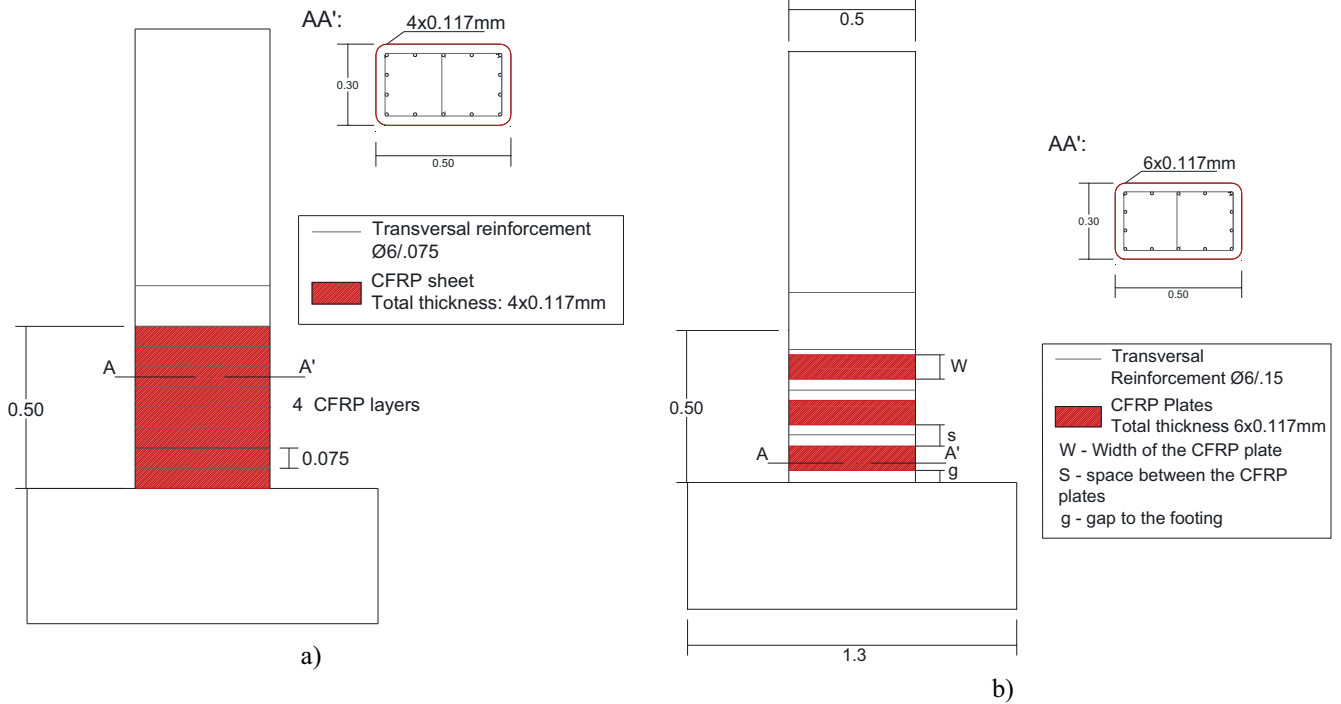


Fig. 4. Repair and retrofit strategies of RC columns a) Stage 3; b) Stage 4; c) and d) Stage 5.

- The stage 5 is composed by rounding of the columns corners and the application of the retrofitting technique which is the CFRP plates and sheet jacketing (Fig. 4c and d). The main difference between both techniques are the application of different number of CFRP plates with certain width, thickness and gap between the footing and the first plate (in the case of the CFRP plates jacketing). In the case of the CFRP sheet jacketing it is adopted a continuous sheet between the foot and the certain height defined according to the predicable plastic joint length

of the column (typically the maximum dimension of the column according to different authors). The plates jacketing allows the concentration of the cracks/damage between the plates, on the other hand the sheet jacketing provides a significant confinement along the plastic hinge length and the cracking pattern appears up than the CFRP sheet height typically.

The final solution adopted for the column PC12N04R was a CFRP sheet jacketing thickness  $t_j = 0.468$  mm, which was materialized by



c)

**Fig. 5.** Repaired and strengthened specimens with CFRP plates jacketing: a) CFRP sheet jacketing design solution adopted; b) CFRP plate jacketing design solution adopted; c) Repaired specimen with CFRP plate jacketing technique general view.

adopting 4 layers, 0.117 mm each one, of CFRP sheets (Fig. 5a). For the columns PC12N05R and PC12N07R was adopted the CFRP plates jacking technique by 3 CFRP plates with 80 mm width, spaced at 70 mm, each one with 6 layers of CFRP sheet thickness of 0.117 mm (total thickness of 0.702 mm), having a 40 mm gap between the footing and the first plate was adopted (Fig. 5b). The mechanical properties of the CFRP adopted for the retrofit process according to the producer are: CFRP elasticity modulus  $E_{fk} = 240000$  MPa; CFRP ultimate strain  $\epsilon_{uj} = 0.0155$  and CFRP ultimate strength  $f_{uj} = 3800$  MPa and the layer thickness of  $t_{jl} = 0.117$  mm.

2.2.2. Group S1 and S2

The strengthening technique adopted for the “as built” RC columns where the CFRP plates and sheet jacking that were designed according to the Priestley et al. design criteria proposed in 1996 [13]. The total CFRP jacking thickness designed were  $t_j = 0.342$  mm and taking into account that the total area along the repaired zone height is given by  $0.342 \times 500 = 171$  mm<sup>2</sup> was then divided by 3 CFRP plates 80 mm wide, spaced at 70 mm, each one with 6 layers of CFRP sheet thickness of 0.117 mm (total thick-

ness of 0.702 mm), having a 40 mm gap between the footing and the first plate (Fig. 5b).

3. Experimental test results

3.1. Shear-drift hysteretic response

The response of the columns were analyzed, namely through the analysis of the shear-drift hysteretic response in both stronger (X) and weaker (Y) direction of the columns. Due to the large number tests, only two examples one of each group are presented in Figs. 6 and 7, however all the discussion refers to some of the test results from an experimental campaign that can be found in [5,6]. The main findings of the experimental campaign were:

- Group R: it was observed that the initial stiffness of the repaired columns were typically equal or lower when compared with the original specimen (in majority of the cases in weak direction), and the yielding occurs for larger drift demands. Regarding the maximum strength, the three repaired tests leads always to larger strength increase in the weak direction than the

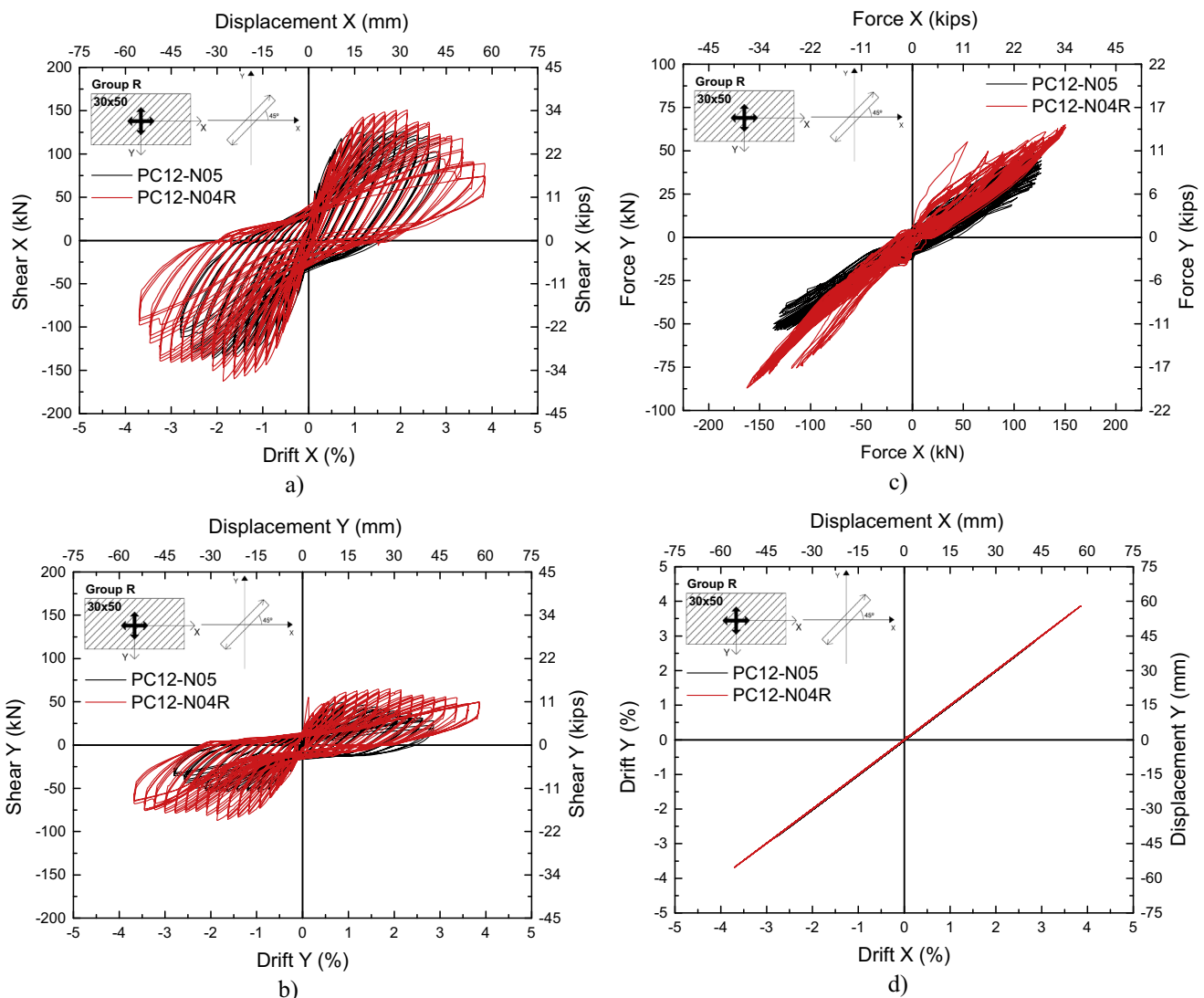


Fig. 6. Specimen PC12N4R from group R results: a) shear-drift (strong direction X); b) shear-drift (weak direction Y); c) Force X-force Y response; d) Drift X- Drift Y response.

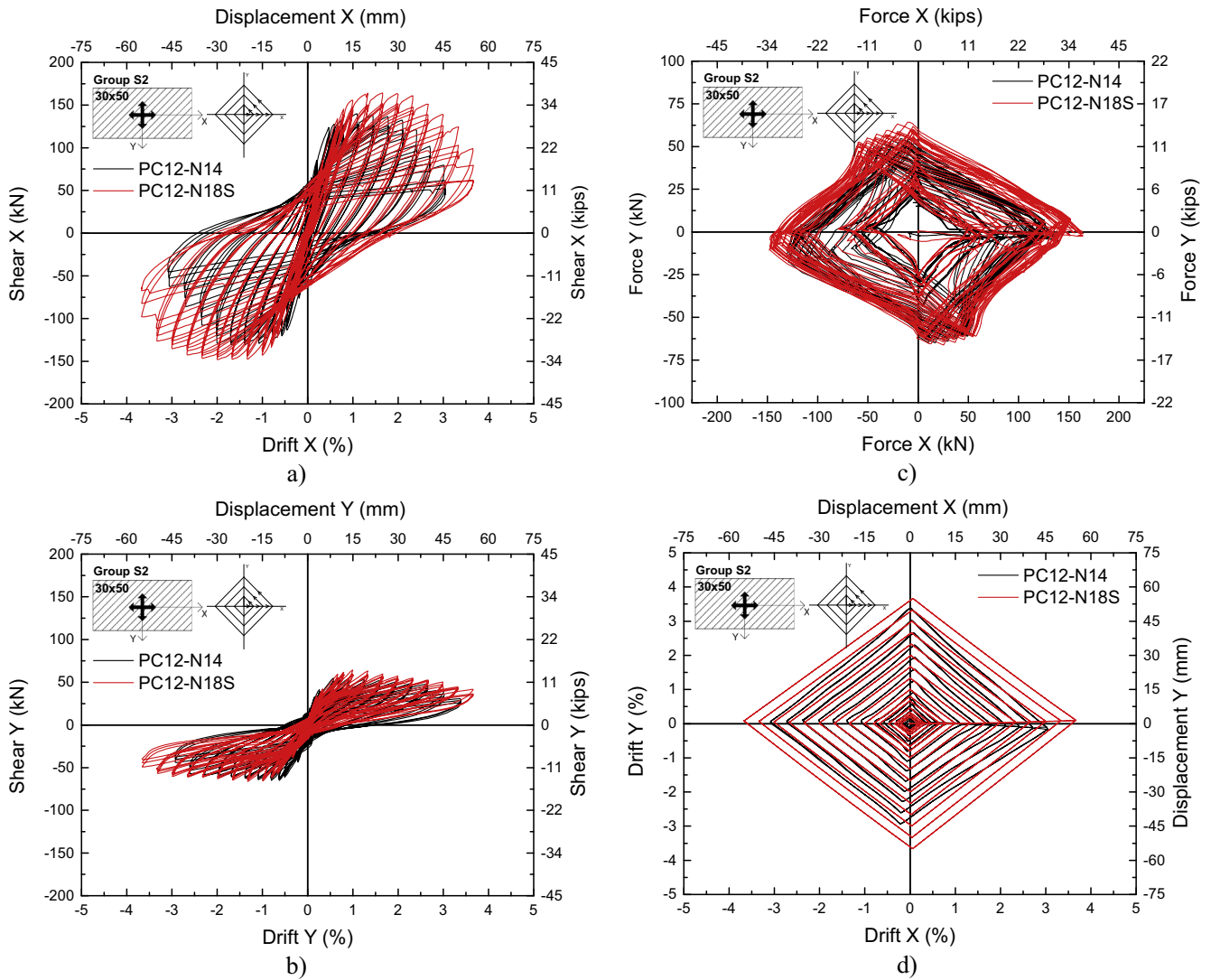


Fig. 7. Specimen PC12N18S from group S2 results: a) shear-drift (strong direction X); b) shear-drift (weak direction Y); c) Force X-force Y response; d) Drift X- Drift Y response.

Table 2  
Maximum and ultimate strength, ultimate displacement and ductility: Group R specimens.

Specimen	Direction	Maximum strength $F_{max}$ (kN)	Ultimate strength $F_u$ (kN)	Ultimate displacement $d_u$ (mm)	Ductility $\mu$
PC12-N05	X	136.8	108.8	41.9	4.25
	Y	66.9	35.5	42.1	5.41
PC12-N04R	X	162.6	97.3	55.5	3.81
	Y	87	66.97	55.2	3.56
PC12-N05R	X	142.8	132.7	44.2	2.99
	Y	75.9	61.24	38.1	2.70
PC12-N07R	X	140.8	132.49	43.1	3.65
	Y	79.5	60.6	39.5	4.29

Table 3  
Maximum and ultimate strength, ultimate displacement and ductility: Group S1 specimens.

Specimen	Direction	Maximum strength $F_{max}$ (kN)	Ultimate strength $F_u$ (kN)	Ultimate displacement $d_u$ (mm)	Ductility $\mu$
PC12-N13	X	136.4	88.4	39.1	4.2
	Y	59.3	29.8	36.3	4.8
PC12-N17S	X	134.9	105.9	40.7	6.7
	Y	54.8	34.5	37.5	4.9

**Table 4**  
Maximum and ultimate strength, ultimate displacement and ductility: Group S2 specimens.

Specimen	Direction	Maximum strength $F_{max}$ (kN)	Ultimate strength $F_u$ (kN)	Ultimate displacement $d_u$ (mm)	Ductility $\mu$
PC12-N14	X	140.0	62.5	43.7	7.5
	Y	64.9	44.1	43.7	7.4
PC12-N10S	X	154.4	97.9	40.9	12.1
	Y	67.5	14.1	69.9	6.1
PC12-N12S	X	157.7	83.9	65.2	3.5
	Y	72.8	41.4	64.9	7.4
PC12-N18S	X	164.3	99.1	54.8	4.6
	Y	66.2	49.2	54.9	5.9

original specimen, around 20%. In the columns strong direction only the specimen PC12-N04R increased significantly the maximum strength value, about 15%. It was observed that the ductility of all the repaired columns was lower than the one of the original column. In Table 2 is summarized the main results in terms of maximum and ultimate strength, ultimate displacement and ductility obtained by each specimen;

- Group S1 and S2: The initial column stiffness, in both directions, were not significantly improved by the CFRP confinement. The maximum strength obtained by the strengthened columns were around 12% higher for all tests with the diamond load path (Group S2). In the tests with the diagonal load path (Group S1) the maximum strength was similar between the “as built” and the strengthened column.. Regarding the specimens ductility it was observed that the specimen PC12-N17S reached higher values, namely 60% in the strong direction X and 3% in the weak direction Y than the “As built column” (Group S1). Globally, the strengthened columns from Group S2 reached higher ductility in their strong direction X, however in the weak direction the same was not observed. In Tables 3 and 4 are summarized the main results in terms of maximum and ultimate strength, ultimate displacement and ductility obtained by each specimen from Group S1 and S2 respectively.

3.2. Cumulative energy dissipation

In the design process of repair and retrofit one of the main purposes is to increase the capacity of the structures increase the energy dissipation capacity when subjected to earthquakes without a significant reduction in strength [26].

The dissipated energy in RC columns subjected to biaxial horizontal loading can be determined considering the dissipated energy in each direction (Eqs. (1) and (2)), and the total energy was calculated as the sum of these two parts, according to Eq. (3).

$$Ed_x = \int F_x d_x \tag{1}$$

$$Ed_y = \int F_y d_y \tag{2}$$

$$Ed_{tot} = \int F_x d_x + \int F_y d_y \tag{3}$$

The evolution of the cumulative energy dissipation for each specimen along the increase of the displacement demand is presented in Fig. 8. The plotted value corresponds to the value of the accumulated dissipated energy at the end of the third cycle of repetition of each displacement peak imposed according to the loading condition defined in sub-section 2.1. From the analysis the results it can be concluded:

- Group R: Through the comparison between as built column (PC12-N05) and the repaired ones it is observed that the CFRP confinement was effective to restore the energy dissipation capacity of the damaged columns and increased the capacity of the specimens PC12-N04R and PC12-N07R about 15% and 56% respectively. The column PC12-N05R was the only one with lower accumulated energy for the same levels of displacement demands, however reached the same energy dissipation than the as built one (Fig. 8a);

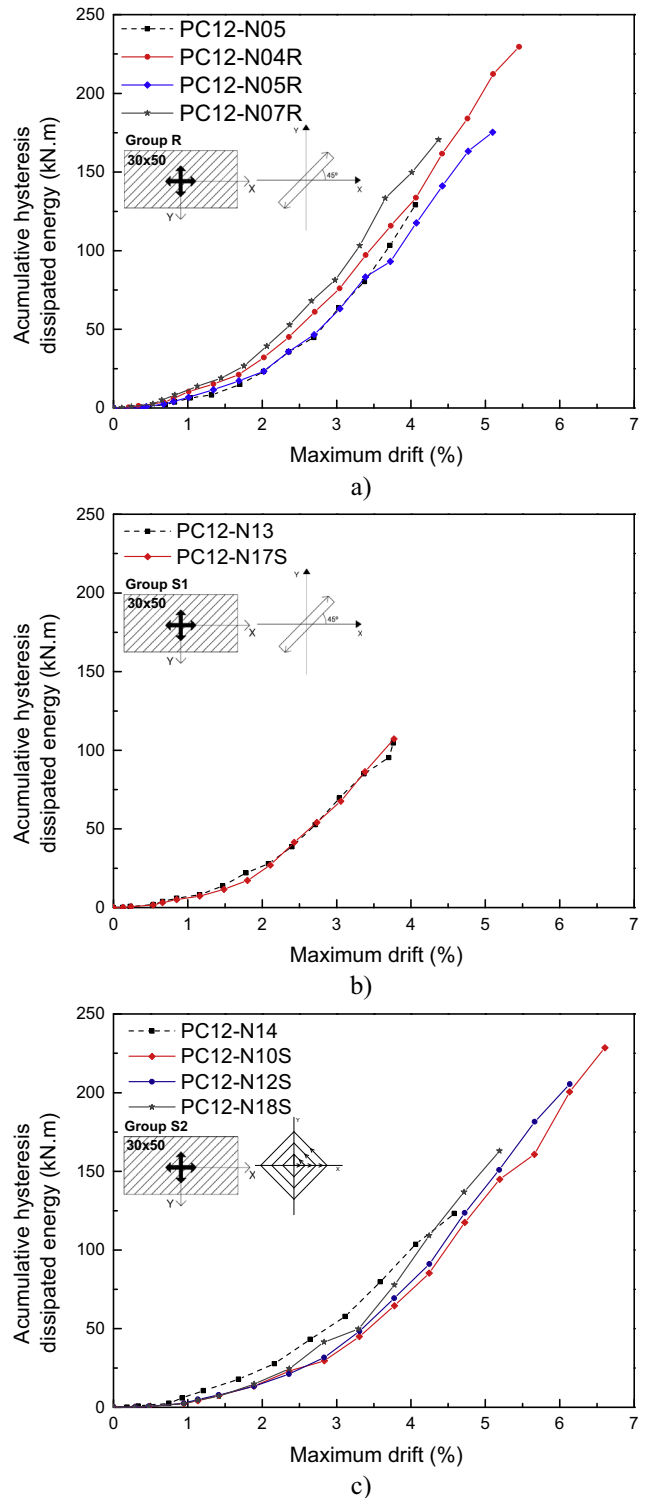


Fig. 8. Cumulative energy dissipation: a) Group R; b) Group S1; and Group S2.

- Group S1: it is observed that the CFRP did not improved significantly the energy dissipation capacity of the specimen PC12-N17S for the same displacement level, which can be due to the concentration of the damage between the CFRP plates. (Fig. 8b);

- Group S2: the results shows that the CFRP confinement improved the energy dissipation capacity of the specimens. All the strengthened columns reached higher total energy dissipation, in particular the specimen PC12-N10S with an increase of about 60%. However it was observed that the strengthened col-

**Table 5**  
Best fit logarithmic curve for global damping for tested each column.

Group	Specimen	Direction	Best fit curve	R <sup>2</sup>
R	PC12-N05	X	$\zeta_{eq} = 84176 \ln(\mu) + 6.4998$	0.9902
		Y	$\zeta_{eq} = 14,807 \ln(\mu) + 0.4762$	0.9503
	PC12-N04R	X	$\zeta_{eq} = 6.7121 \ln(\mu) + 8.8367$	0.9359
		Y	$\zeta_{eq} = 2.5059 \ln(\mu) + 13.405$	0.7681
	PC12-N05R	X	$\zeta_{eq} = 7.6259 \ln(\mu) + 8.6673$	0.9764
		Y	$\zeta_{eq} = 3.3233 \ln(\mu) + 5.7034$	0.3812
	PC12-N07R	X	$\zeta_{eq} = 7.6259 \ln(\mu) + 8.7136$	0.9764
		Y	$\zeta_{eq} = 11.0151 \ln(\mu) + 5.7034$	0.9405
S1	PC12-N13	X	$\zeta_{eq} = 8.3704 \ln(\mu) + 5.9968$	0.9305
		Y	$\zeta_{eq} = 12.737 \ln(\mu) + 4.2023$	0.9186
	PC12-N17S	X	$\zeta_{eq} = 9.0937 \ln(\mu) + 4.4609$	0.9706
		Y	$\zeta_{eq} = 14.407 \ln(\mu) + 6.1196$	0.9604
S2	PC12-N14	X	$\zeta_{eq} = 11.406 \ln(\mu) + 6.4399$	0.928
		Y	$\zeta_{eq} = 6.0601 \ln(\mu) + 6.3664$	0.7822
	PC12-N10S	X	$\zeta_{eq} = 10.519 \ln(\mu) + 5.3135$	0.8506
		Y	$\zeta_{eq} = 5.1746 \ln(\mu) + 6.6499$	0.746
	PC12-N12S	X	$\zeta_{eq} = 11.549 \ln(\mu) + 4.5573$	0.7034
		Y	$\zeta_{eq} = 3.3023 \ln(\mu) + 9.2964$	0.2307
	PC12-N18S	X	$\zeta_{eq} = 15.721 \ln(\mu) + 2.7241$	0.9794
		Y	$\zeta_{eq} = 2.4937 \ln(\mu) + 7.5066$	0.3009

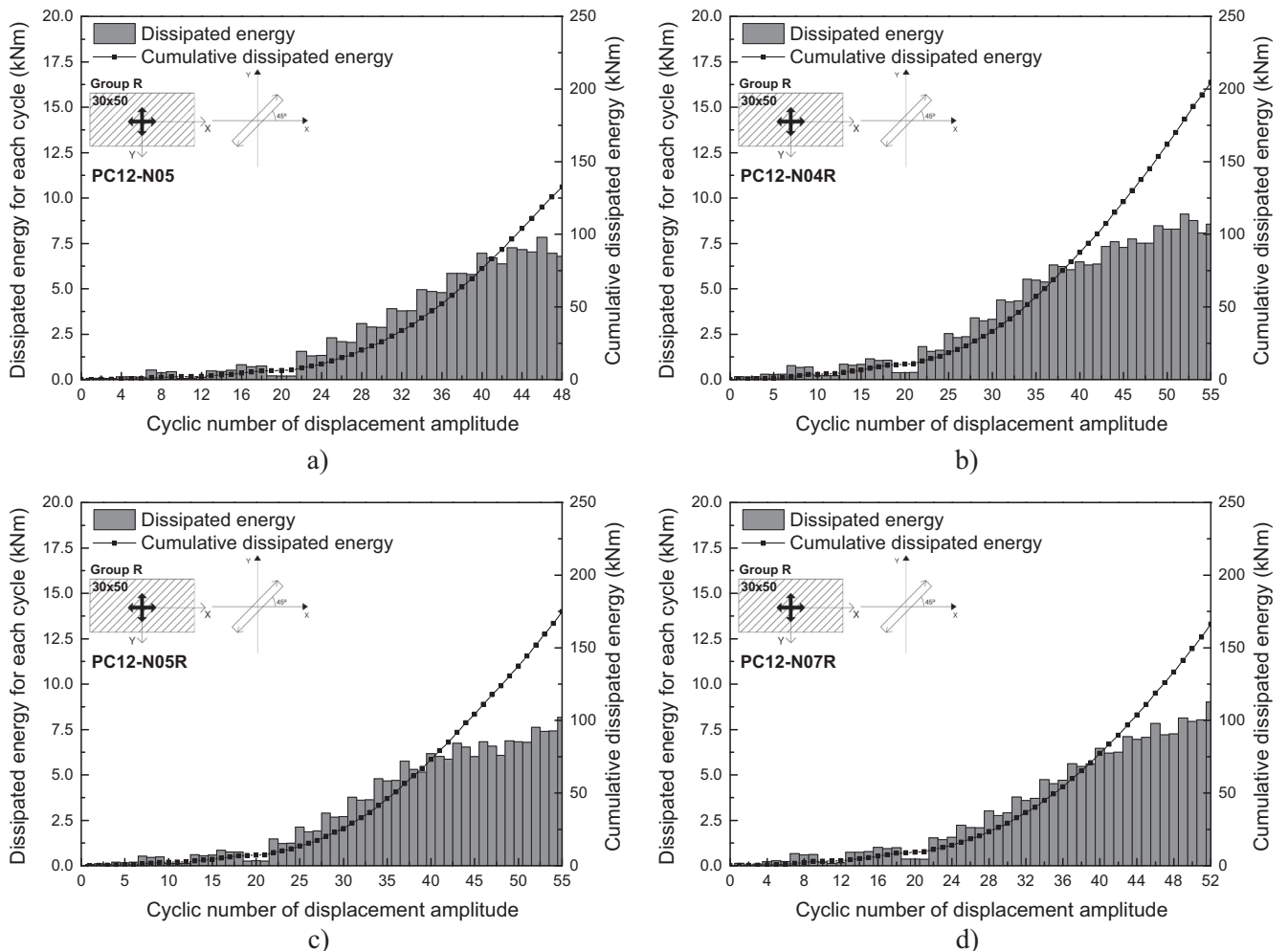


**Fig. 9.** Dissipated energy for each cycle for Group R columns: a) PC12-N05; b) PC12-N04R; c) PC12-N05R and; d) PC12-N07R.

umns dissipated equal or lower energy than the “as built” column for the same displacement demand. however the all the strengthened columns subjected to the diamond displacement path reached higher energy dissipation values, namely the specimen PC12-N10S obtained 80% more energy dissipation and the PC12-N18S with only 10% (Fig. 8c).

In comparison with the experimental study conducted by Real-fonzo and Napoli [27] that was performed to evaluate the efficiency of CFRP jacketing to improve the uniaxial cyclic behaviour of high aspect ratio RC columns. They observed in all the strengthened specimens the increase of energy dissipation provided by the CFRP confinement. Which did not occur in the present experimen-

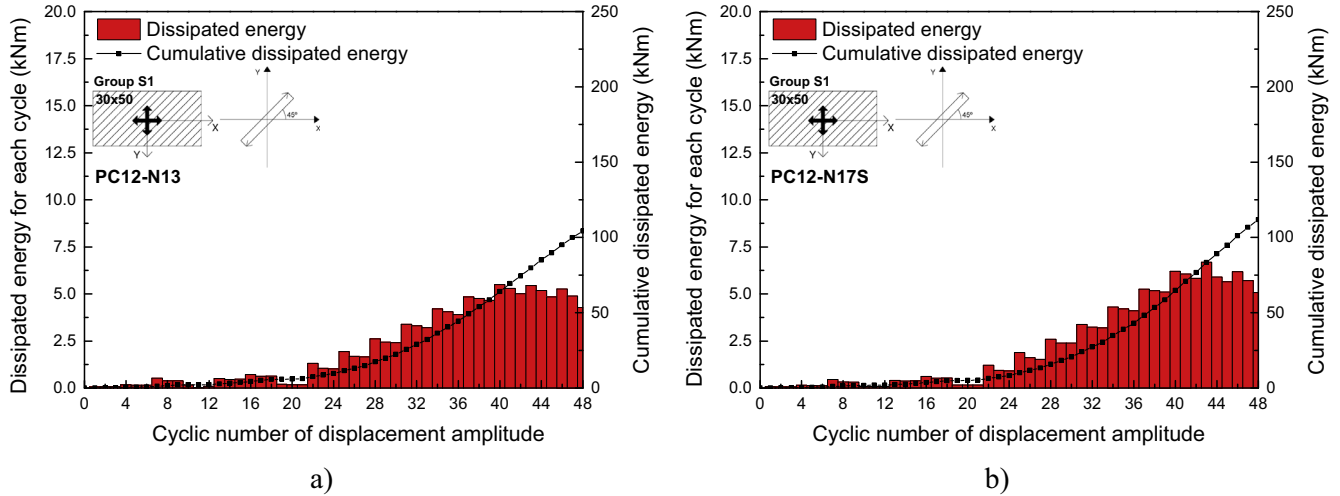


Fig. 10. Dissipated energy for each cycle for Group S1: a) PC12-N13; b) PC12-N17S.

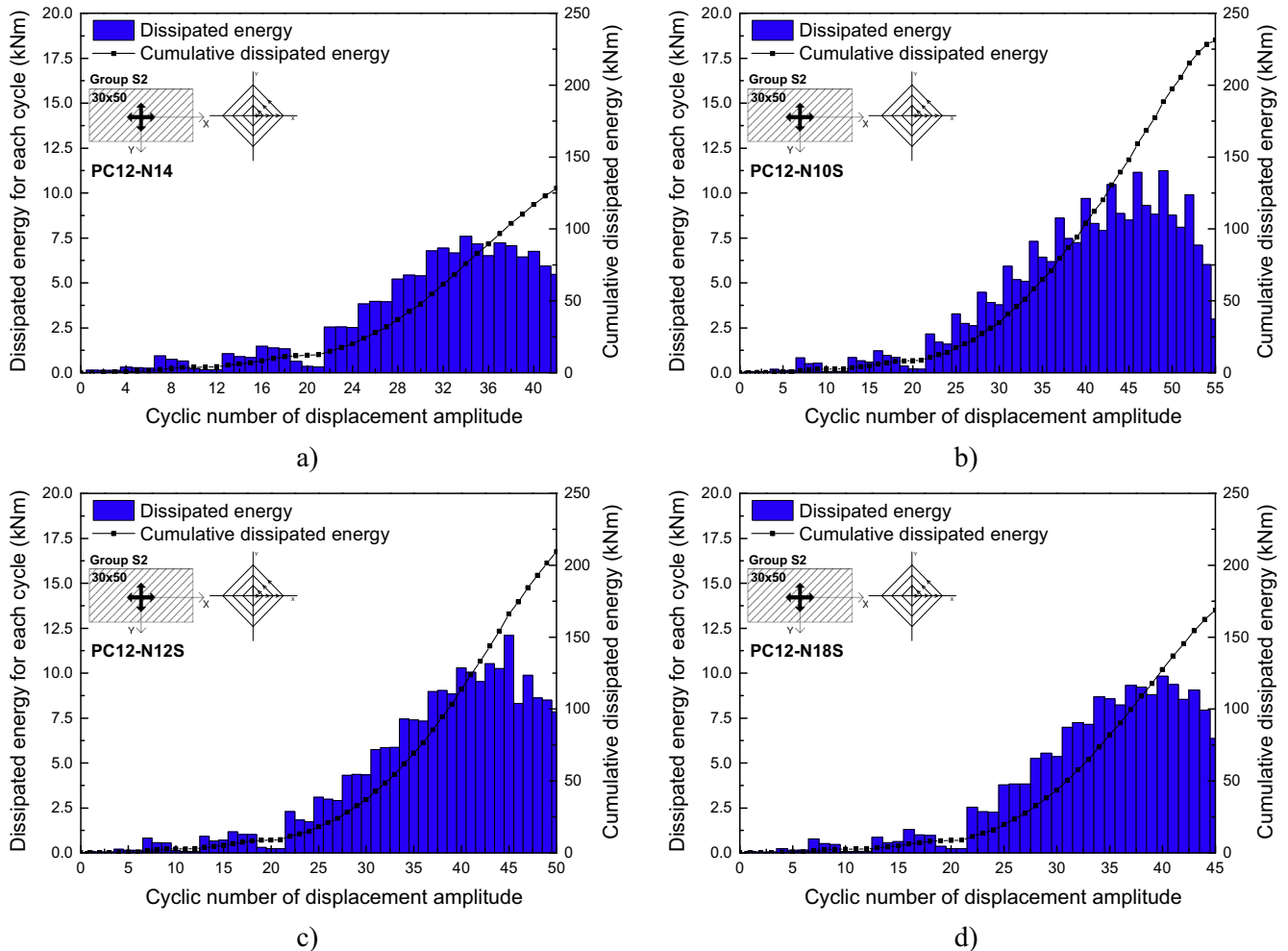


Fig. 11. Dissipated energy for each cycle for Group S2: a) PC12-N14; b) PC12-N10S; c) PC12-N12S; and d) PC12-N18S.

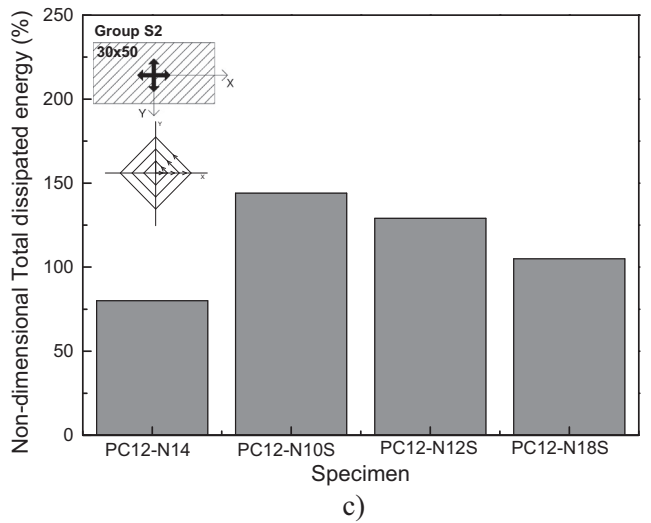
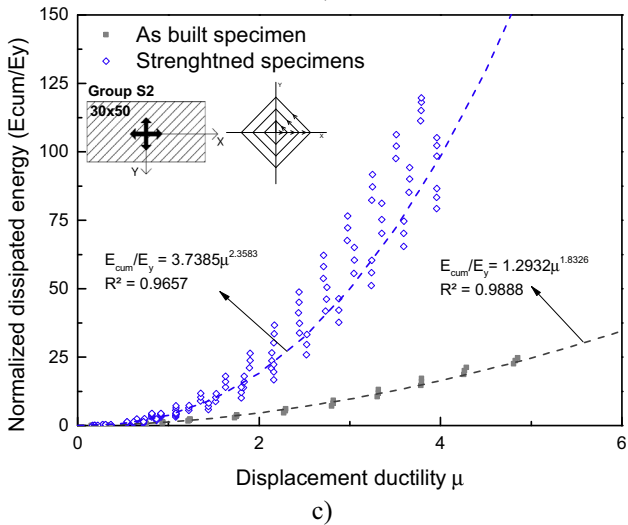
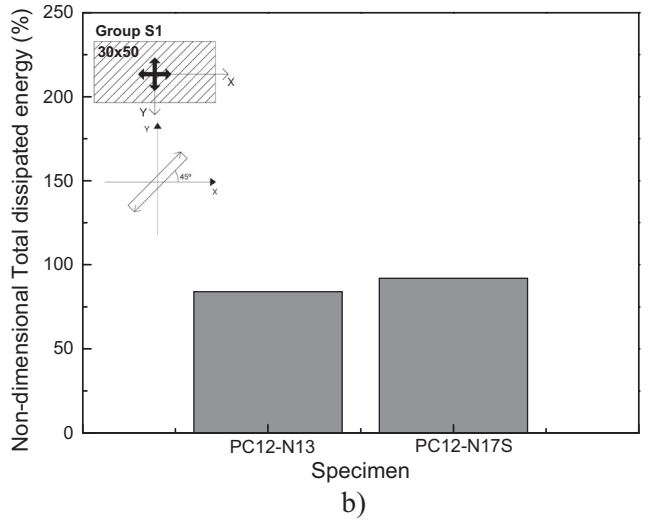
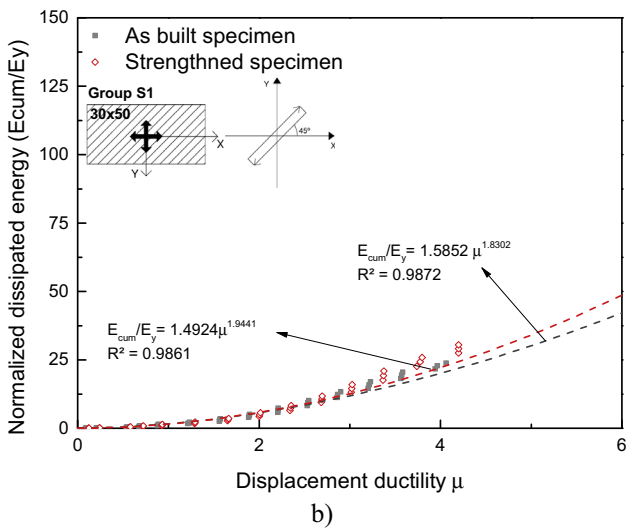
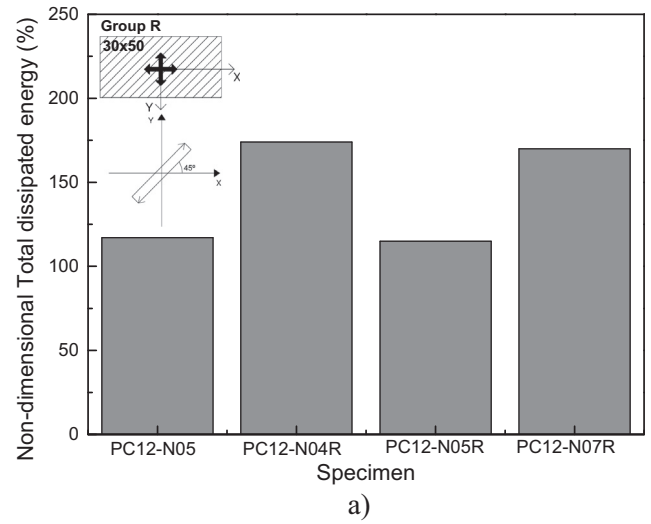
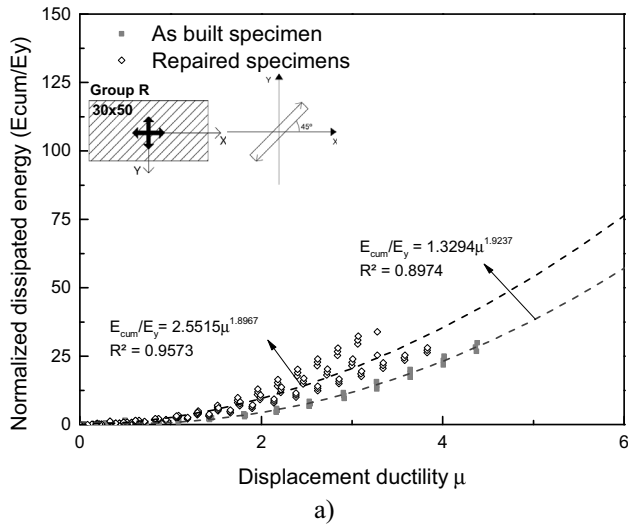


Fig. 12. Normalized dissipated energy: a) Group R; b) Group S1; and c) Group S2.

Fig. 13. Evaluation of total energy dissipated for columns: a) Group R; b) Group S1; and c) Group S2.

tal campaign for the same displacement demands. Globally the strengthened RC columns (Group S1 and S2) dissipated similar or lower energy when compared to the results of the original specimens, for the same displacement demands due to the concentration of the damage along the test (Table 5).

### 3.3. Individual energy dissipation for each cycle

The energy dissipated for each individual loading cycle and the accumulated energy dissipation along each tested column was cal-

culated. In Figs. 9–11 are presented the Group R, S1 and S2 results respectively. From the analysis of the results obtained for the tested columns, the following can be concluded:

- As observed by other authors [1], the 1st cycle of each peak displacement, dissipated more energy than the subsequent cycles with the same peak displacement. In the Group R (Fig. 9) columns, no significant difference between the “as built” column and the repaired ones was observed, however for the Group S1 (Fig. 10) and S2 (Fig. 11) the reduction of the dissipated energy in the 2nd and 3rd cycles is about 5% and 20% of the energy dissipated in the 1st cycle respectively. It is clear that more reduction is observed in the Group S2 and could be caused by the damage induced during the 1st cycle that reduces the stiffness and strength, thus decreasing the energy dissipation capacity of the column in the 2nd and 3rd cycles;
- No significant drop in the energy dissipation for higher drift demands for the Group R and S1 specimens, however for the Group S2 strengthened specimens it is observed a 15% reduction of the dissipated energy per cycle.

### 3.4. Normalized dissipated energy

For each specimen, the energy dissipation determined was normalized with the total dissipated energy until the first yield point ( $E_y$ ), and are plotted in Fig. 12. It was found some differences between the “as built” columns and the repaired and strengthened ones, as can be observed through the best-fit power correlation curves extracted for all tests expressed in Eqs. (4)–(9):

$$\frac{E_{cum}}{E_y}_{GroupR,Asbuilt} = 1.3294 \times \mu^{1.9237} \quad (4)$$

$$\frac{E_{cum}}{E_y}_{GroupR,Repaired} = 2.5515 \times \mu^{1.8967} \quad (5)$$

$$\frac{E_{cum}}{E_y}_{GroupS1,Asbuilt} = 1.5852 \times \mu^{1.8302} \quad (6)$$

$$\frac{E_{cum}}{E_y}_{GroupS1,Strengthened} = 1.4924 \times \mu^{1.9441} \quad (7)$$

$$\frac{E_{cum}}{E_y}_{GroupS2,Asbuilt} = 1.2932 \times \mu^{1.8326} \quad (8)$$

$$\frac{E_{cum}}{E_y}_{GroupS2,Strengthened} = 3.7385 \times \mu^{2.3583} \quad (9)$$

where  $E_{cum}$  is the accumulative energy dissipation and  $\mu$  is the columns displacement ductility.

From the results it can be observed a significant effect of the CFRP confinement in Group R and S2 specimens. Namely from the proposed expressions it was observed that the normalized dissipated energy value for the same displacement ductility is 2–3 times higher, when comparing the Group S2 strengthened columns and the as built one, 2 times higher for the Group R repaired columns and the as built one which is associated with the efficiency of the CFRP plates jacketing. However, as observed before no effect due to the CFRP confinement was observed to the specimen PC12-N17S (Group S1), which could be associated to the displacement load path (diagonal 45°) that past researches showed to have an important influence in the reduction of the columns capacity [4]. This fact associated to some concentration of the damaged due to the CFRP confinement could lead to a poor performance of the column PC12-N17S. Further experimental testes are necessary to validate that the diagonal 45° displacement path could reduce the improvement provided by the CFRP confinement and to found a

validated expression such for repaired columns and for strengthened columns, which would be very useful to estimate the dissipated energy in the seismic design of RC elements retrofitted.

### 3.5. Total dissipated energy

Fig. 13 compared the total dissipated energy obtained from the test results. This total dissipated energy corresponds to the energy dissipated from the start of the test until conventional rupture is reached, to a strength decay of 20% relative to the maximum strength. From the analysis of the results, the following observations can be drawn:

- Group R: all the repaired columns dissipated more energy when compared with the as built one, namely the PC12-N04R dissipated 60% more energy and PC12N05R only more 2%;
- Group S1 and S2: regarding the columns of Group S1 it is observed that PC12-N17S dissipated 5% more energy than the as built one. The strengthened columns of the group S2 dissipated more between 25% and 75% for the columns PC12-N10S and PC12-N18S respectively.

### 3.6. Equivalent damping

The equivalent damping depends on the structural displacement ductility demand and the location of the plastic hinges in the elements [28] and can be defined by the sum of the elastic and hysteretic damping given (see Eq. (10)). Elastic damping ( $\zeta_{el}$ ) is typically considered to be 5% for RC structures, related to the critical damping [29].

$$\zeta_{eq} = \zeta_{el} + \zeta_{hyst} \quad (10)$$

The equivalent hysteretic damping coefficient ( $\zeta_{hyst}$ ) can be obtained by Eq. (11), where  $E_D$  and  $A_{loop}$  are the shaded area shown in Fig. 14, corresponding to the dissipated energy; where  $E_{S0}$  is the strain energy, and  $F_{max}$  and  $D_{max}$  are the maximum force and displacement achieved in the loop.

$$\zeta_{hyst} = \frac{E_D}{4\pi E_{S0}} = \frac{A_{loop}}{2\pi F_{max} D_{max}} \quad (11)$$

For each tested column the equivalent damping was calculated, according to the presented methodology, for each independent direction (X and Y) from the shear-drift curves. Subsequently a

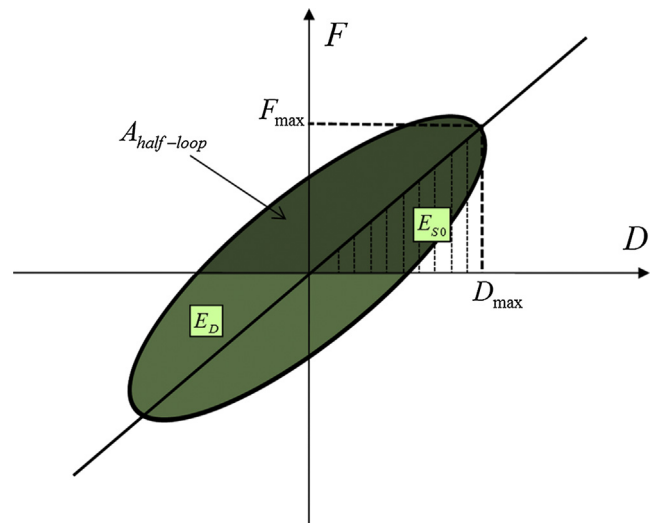


Fig. 14. Example of damping determination for a hysteretic half-cycle.

best-fit logarithmic curve was adjusted for each tested column in terms of equivalent damping as a function of maximum ductility demand as performed by Rodrigues [1].

Fig. 15 allow comparing the best-fit logarithmic curves obtained for each tested column and each direction (X and Y) while the equations and the correlation factors ( $R^2$ ) are summarized in Table 2. In particular, Fig. 15 shows the results for the different groups. From the results analysis of the in terms of the equivalent damping function of ductility it is possible to verify that:

- The logarithmic best-fit curve correlates well with test results for the as built tests, but slight lower correlation factors were found from the Group R and S1 test results;
- A significant reduction of the correlation factor was observed for the weak direction, in particular for the Group S2 results;
- From the Group R results it is possible to observe higher equivalent damping results of the as built test, compared with the repaired ones in the weak direction. In the strong direction the equivalent damping of all the tests are similar;

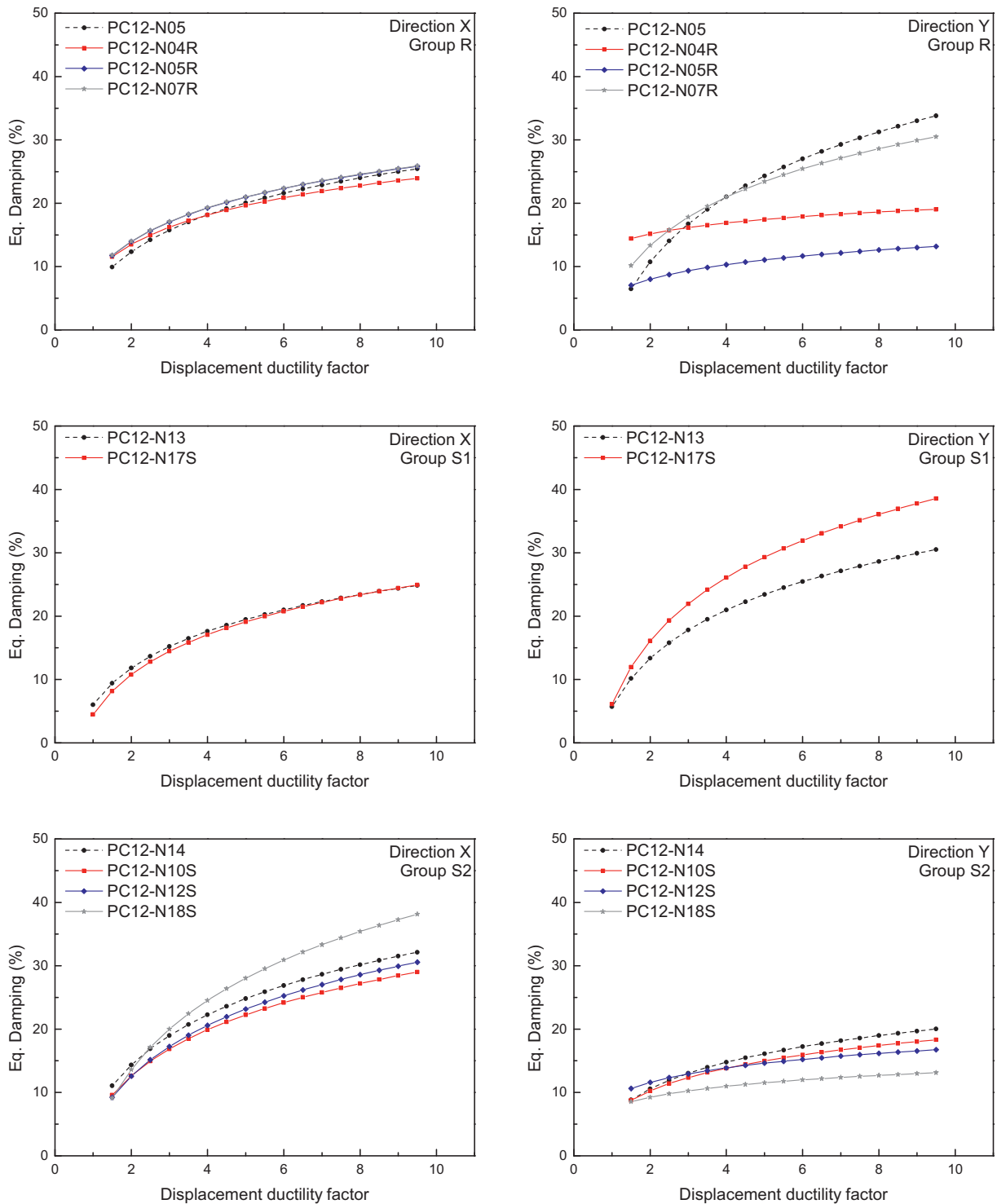


Fig. 15. Best-fit equivalent damping vs. maximum ductility demand for: Group R, S1 and S2.

- From the Group S1 results it is possible to observe that in the strong direction the equivalent damping of both columns are similar, however for the weak direction the strengthened column reached higher equivalent damping;
- From the Group S2 it is possible to observe similar equivalent damping values between the strengthened columns and the as built one in the strong direction, however in the weak direction the as built column reached higher equivalent damping values.

Different proposals for the equivalent damping of RC elements and structures can be found in the literature, including the works of Priestley et al. [30,31], Rosenblueth and Hererra [32], Gulkan and Sozen [33], Kowalsky [34], among others. Blandon [35] developed an extensive review and study of the existing proposals for all type of elements. The more frequently used equations for predicting the equivalent damping ( $\xi$ ) of RC columns as a function of ductility ( $\mu$ ) are the following:

Priestley [30], for concrete columns and walls:

$$\xi_{eq} = 5 + \frac{95}{\pi} \left( 1 - \frac{1}{\sqrt{\mu}} \right) \quad (12)$$

Priestley et al. [36], for concrete framed buildings

$$\xi_{eq} = 0.05 + 0.565 \left( \frac{\mu - 1}{\mu\pi} \right) \quad (13)$$

The results given by the presented equations were compared with the experimental results obtained from the tests. In order to evaluate the accuracy of the presented empirical expressions, the correlation factor between the predicted values and the experimental results has been calculated. From an analysis of the results, using the strengthened test data the Equation 10 show better correlation with the experimental results ( $R^2 > 0.8$ ) (Fig. 16).

Additionally it is proposed an empirical equation (Eq. (14)) to obtain the equivalent damping for repaired and strengthened RC columns with CFRP confinement with good approximation with the experimental results ( $R^2 = 0.75$ ). The obtained expression present a good correlation with the experimental results. The methodology adopted to obtain the expression was based on past approaches proposed by different authors in the literature [1,17,35] namely through a logarithmic curve that match the best-fit logarithmic curves obtained for each tested column and for each direction. As reported in the literature for very low ductil-

ity values the viscous damping is usually reported as 5 [1,17,35]. The expression presented gives an important difference for low ductility factors, once the experimental results are clearly higher than the ones obtained by theoretical expressions and gives similar values to the ones proposed by Priestly et al. [30,31] for ductility factors between 2 and 4.

$$\xi_{eq} = 10.92 \ln(\mu) + 5 \quad (14)$$

#### 4. Summary and conclusions

In the Laboratory of Earthquake and Structural Engineering it was carried out an experimental campaign on 10 RC columns subjected to biaxial horizontal loading combined with constant axial load, three of them were subjected to repair process in order to restore the original capacity of the columns and four of them were strengthened in order to improve the original capacity. For both of them it was used the CFRP plates jacketing in the retrofit process. Based on the results, the following conclusions can be drawn:

- It was observed that the repair strategy restored the energy dissipation capacity of the damaged columns, and all the repaired columns reached the as built dissipated energy. Regarding the strengthened columns, it was observed that the use of CFRP jacketing in as built columns improved about 10%-20% the energy dissipation capacity of all the columns for larger drift demands;
- An expression relating the RC element's displacement ductility and normalized dissipated energy was proposed for strengthened and repaired columns subjected to biaxial loading and constant axial force;
- From the analysis of the viscous damping of each independent direction of columns, it was observed that in the weak direction the strengthened columns reached lower equivalent damping values than the original one and higher values for the repaired columns;
- Different proposals, already available in the literature, for the prediction of equivalent damping of RC columns under uniaxial loading were compared with the experimental results, showing that some of expressions suggested by Priestley could represent satisfactory the results obtained for the strengthened columns;

This research work is expected to contribute towards a better understanding of the biaxial response of repaired and strengthened RC columns with CFRP jacketing and for the calibration of suitable numerical models for the representation of their biaxial lateral response under cyclic loading reversals.

#### References

- [1] Rodrigues H, Varum H, Arêde A, Costa A. A comparative analysis of energy dissipation and equivalent viscous damping of RC columns subjected to uniaxial and biaxial loading. *Eng Struct* 2012;35:149–64.
- [2] Rodrigues H, Arêde A, Varum H, Costa A. Experimental evaluation of rectangular reinforced concrete column behaviour under biaxial cyclic loading. *Earthquake Eng Struct Dynam* 2013;42:239–59.
- [3] Rodrigues H, Arêde A, Varum H, Costa A. Damage evolution in reinforced concrete columns subjected to biaxial loading. *Bull Earthq Eng* 2013;11:1517–40.
- [4] Rodrigues H, Furtado A, Arêde A. Behavior of rectangular reinforced-concrete columns under biaxial cyclic loading and variable axial loads. *J Struct Eng* 2016;142.
- [5] Rodrigues H, Arêde A, Furtado A, Rocha P. Seismic behavior of strengthened RC columns under biaxial loading: an experimental characterization. *Constr Build Mater* 2015;95:393–405.
- [6] Rodrigues H, Arêde A, Furtado A, Rocha P. Seismic rehabilitation of RC columns under biaxial loading: an experimental characterization. *Structures* 2015;3:43–56.
- [7] Priestley MJN, Park R. Strength and ductility of concrete bridge columns under seismic loading. *ACI Struct J* 1987;84:61–76.

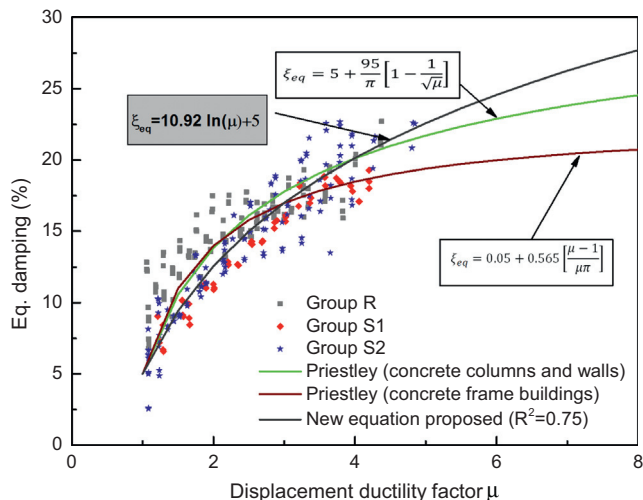


Fig. 16. Equivalent damping estimated with empirical expressions, including a new empirical equation proposed and results for Group R, S1 and S2.

- [8] Priestley M, Seible F, Calvi M. Seismic design and retrofit of bridges. New York: Wiley; 1996.
- [9] Seible F, Priestley M, Hegemier G, Innamorato D. Seismic retrofit of RC columns with continuous carbon fiber jackets. *J Compos Constr* 1997;1:52–62.
- [10] Monti G, Nisticó N, Santini S. Design of FRP jackets for upgrade of circular bridge piers. *J Compos Constr* 2001;5:94–101.
- [11] Meda A, Mostosi S, Rinaldi Z, Riva P. Corroded RC columns repair and strengthening with high performance fiber reinforced concrete jacket. *Mater Struct* 2016;49:1967–78.
- [12] Alcocer S. RC frame connections rehabilitated by jacketing. *J Struct Eng* 1993;119:1413–31.
- [13] Júlio E, Branco F. Reinforced concrete jacketing-interface influence on cyclic loading response. *ACI Struct J* 2008;1–7.
- [14] Júlio E, Branco F, Silva V. Structural rehabilitation of columns with reinforced concrete jacketing. *Prog Struct Mat Eng* 2003;5:29–37.
- [15] Belal MF, Mohamed HM, Morad SA. Behavior of reinforced concrete columns strengthened by steel jacket. *HBRC J* 2015;11:201–12.
- [16] Ghobarah A, Biddah A, Mahgoub M. Rehabilitation of reinforced concrete columns using corrugated steel jacketing. *J Earthquake Eng* 1997;1:651–73.
- [17] Varum H. Seismic assessment, strengthening and repair of existing buildings (Ph.D. thesis). Aveiro: Departamento de Engenharia Civil, Universidade de Aveiro; 2003.
- [18] Ozcan O, Binici B, Ozcebe G. Seismic retrofitting of reinforced concrete columns using carbon fiber reinforced polymer (CFRP). In: Presented at the Asia-Pacific conference on FRP in structures (APFIS 2007); 2007.
- [19] Punurai W, Hsu C, Punurai S, Chen J. Biaxially loaded RC slender columns strengthened by CFRP composite fabrics. *Eng Struct* 2013;46:311–21.
- [20] Tahsiri H, Sedehi O, Khaloo A, Raisi E. Experimental study of RC jacketed and CFRP strengthened RC beams. *Constr Build Mater* 2015;95:476–85.
- [21] Tsonos A. Effectiveness of CFRP-jackets and RC-jackets in post-earthquake and pre-earthquake retrofitting of beam-column subassemblages. *Eng Struct* 2008;30:777–93.
- [22] Yalein C, Kaya O, Sinangil M. Seismic retrofitting of R/C columns having plain rebars using CFRP sheets for improved strength and ductility. *Constr Build Mater* 2008;22:295–307.
- [23] Ye L, Zhang K, Zhao S, Feng P. Experimental study on seismic strengthening of RC columns with wrapped CFRP sheets. *Constr Build Mater* 2003;17:499–506.
- [24] Lu B, Silva PF. Estimating equivalent viscous damping ratio for RC members under seismic and blast loadings. *Mech Res Commun* 2006;33:787–95.
- [25] Shibata A, Sozen M. Substitute-structure method for seismic design in R/C. *J Struct Div* 1976;102:1–18.
- [26] Elmenhawi A, Brown T. Hysteretic energy and damping capacity of flexural elements constructed with different concrete strengths. *Eng Struct* 2010;32:297–305.
- [27] Realfonzo R, Napoli A. Results from cyclic tests on high aspect ratio RC columns strengthened with FRP systems. *Constr Build Mater* 2012;37:606–20.
- [28] Priestley MJN. Displacement-based seismic assessment of reinforced concrete buildings. *J Earthquake Eng Imperial College London* 1997;1:157–92.
- [29] Priestley MJN, Calvi GM, Kowalsky MJ. Direct displacement-based seismic design of structures. Pavia: IUSS Press; 2007.
- [30] Priestley MJN. Myths and Fallacies in Earthquake Engineering, Revisited" The Mallet Milne Lecture. Italy.: IUSS Press, Pavia; 2003.
- [31] Priestley MJN, Calvi MJ, Kowalsky MJ. Displacement-based seismic design of structures. IUSS Press; 2007.
- [32] Rosenblueth E, Herrera I. On a kind of hysteretic damping. *J Eng Mech Div ASCE* 1964;90:37–48.
- [33] Gulkan P, Sozen A. Inelastic responses of reinforced concrete structures to earthquake motions. In: Proceedings of the ACI, vol. 71, No. 12; 1974.
- [34] Kowalsky MJ. Displacement based design – a methodology for seismic design applied to RC bridge columns [MSc thesis]. California: University of California, San Diego; 1994.
- [35] Blandon C. Equivalent Viscous Damping Equations for Direct Displacement Based Design. Rose School, Pavia: Master; 2004.
- [36] Priestley MJN, Calvi MJ, Kowalsky MJ. Displacement-based seismic design of structures. IUSS Press; 2007.